Soldering and Packaging Study for an Optical Filter Required for High Resolution Earth Observation Space Missions

Mariia Kepper[1,2], Pol Ribes-Pleguezuelo[1], Marcel Hornaff[1], Erik Beckert[1], Ramona Eberhardt[1], Pascal Pranyies[3], Isabelle Toubhans[3], Francis Descours[3] and Andreas Tünnermann[1]
[1]*Fraunhofer Institute for Applied Optics and Precision Engineering IOF, Albert-Einstein-Str. 7, 07745 Jena, Germany*
[2]*Friedrich Schiller University Jena, Abbe School of Photonics, Albert-Einstein-Straße 6, 07745 Jena, Germany*
[3]*Sodern, 20 Avenue Descartes, 94451 Limeil-Brevannes, France*

Keywords: Optical Filter, Solderjet Bumping Technique, Space, Satellite, Earth Observation.

Abstract: The goal of our study is to optimize the packaging process of an optical sensor module under the space mission requirements. The intention of the project is to develop a generation of optical sensor modules avoiding conventional organic adhesives (standard used technologies). The sensor module, designed by Sodern, consists of three parts: the sensor, the filter frame and the filter. The Solderjet Bumping is planned to be used for assembling KOVAR(29 % Ni, 17 % Co, 54 % Fe) and N-BK10 (Borosilicate-Kronglas, Schott glass) and for assembling KOVAR and KOVAR materials, chosen for this application, and creation of a strong bond between these materials, which should withstand the harsh environmental space conditions.

1 INTRODUCTION

1.1 Motivation

Earth Observation (EO) missions with the objective to inspect the Earth with the help of High Resolution (HR) Systems devices play a leading role in our days. These types of scanner devices are regularly used for passive remote sensing from the space. The trend of the improvement of spatial resolution could be seen on the example of the previous generation of the satellite - Pleiades program– in the decrease of the ground sampling distance from 2.8 m to 0.3 m (Le Goff et al., 2006; Airbus, 2017). These scanning systems have a significant impact not only on the needs of the civilian and defence users but also on the institutional and commercial ones like non-military observations of the oceans or meteorological forecasts (Gleyzes and Perret, 2013).

However, operating on the orbit, the focal plane of the construction have to manage with the variation of the detector module power dissipation while achieving a superb quality of the image. The process of the manufacturing of a better focal plane in the goal of establishing the coverage of a wide swath over the ground is accomplished by abutting of the detection modules. The system miniaturisation requires the optimisation of the optical setup in terms of the simplifying the focal plane arrangement with a far better-staggered positioning of the modules, which involves a mosaic configuration of the filter sensors in the focal plane (Pranyies et al., 2018).

In this paper, an optical filter, suitable for this strategic space aim, is assembled using the soft solder alloys (applied by the Solderjet Bumping technique) instead of the organic adhesives as a bonding agent (Figure 1).

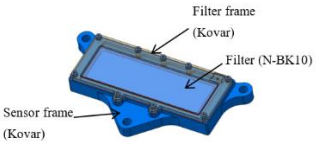

Figure 1: The schematic filter design.

The construction of the filter package consists of two assemblies fabricated by different materials: KOVAR (29 % Ni, 17 % Co, 54 % Fe) and N-BK10 (Borosilicate-Kronglas, Schott glass). To bond this system, a special layer of interconnection is required. Adhesive bonding as a relevant technology in the process of joining the different components into one common assembly, unfortunately, presents a number of several disadvantages, such as molecular pollution

Kepper, M., Ribes-Pleguezuelo, P., Hornaff, M., Beckert, E., Eberhardt, R., Pranyies, P., Toubhans, I., Descours, F. and Tünnermann, A.
Soldering and Packaging Study for an Optical Filter Required for High Resolution Earth Observation Space Missions.
DOI: 10.5220/0007525100850093
In *Proceedings of the 7th International Conference on Photonics, Optics and Laser Technology (PHOTOPTICS 2019)*, pages 85-93
ISBN: 978-989-758-364-3

(due to outgassing in the vacuum that results in the laser-induced contamination and laser-induced damage, Ribes 2018), ionic pollution (damaging for microelectronics ships), shorter lifetimes (organic components) and potential device misalignment (Brockmann et al., 2009; Wernham et al., 2010; Wagner, 2014). Laser-based Solderjet Bumping offers an alternative to this standard technology due to the solid advantages of using an inorganic solder alloy. Thus, it is investigated as a new assembling technique for such devices. It allows operation of the filter in a broad temperature range (from -40°C to 60°C) with high reliability and a long lifetime (Ribes et al., 2018, 2016). The thermal impact is very well controlled and localised compared to the commonly used reflow soldering techniques. The laser energies (required to precisely melt the soldering agent and to bond correctly different materials by creating little thermo-mechanical stress on the components) are adjusted via the combination of the parameters, such as the laser current and the pulse duration.

1.2 Solderjet Bumping Technique

The Solderjet Bumping technology, used for flip-chip assembly in the electronics industry, was adapted by Fraunhofer IOF for assembling optical components as the required modular device. Laser soldering techniques provide good thermal contact between the solder alloy and the surface of the sample. The samples, however, require a wettable surface.

The term wetting carries a meaning of a fluid dynamic process of a liquid displacing another fluid along the solid surface. It can be defined by a position and angle created by a spherical soldering alloy applied onto a selected planar surface (Figure 2, Puttlitz and Stalter, 2004).

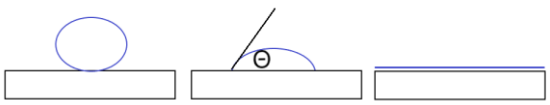

Figure 2: From left to right: non-wetting (Θ>90°), partial wetting, completely wetted solid (Θ=0°) (Puttlitz and Stalter, 2004).

The Solderjet Bumping bond head uses solder spheres (ranging between 40-760 µm diameters) located in a reservoir, got singulated and transported from the alloy reservoir to the jet capillary by a singulation disk and gravitational force. The tip diameter of this capillary is slightly smaller than the initial diameter of the spheres, so the sphere is stuck at the capillary tip (Ribes et al., 2018). Finally, with the help of the infrared laser pulse and under the nitrogen pressure, the solder alloy is heated to melting temperatures and ejected out of the capillary onto the required material (Figure 3). The laser energy is precisely controlled by the laser current (A) and the laser pulse (ms) parameters.

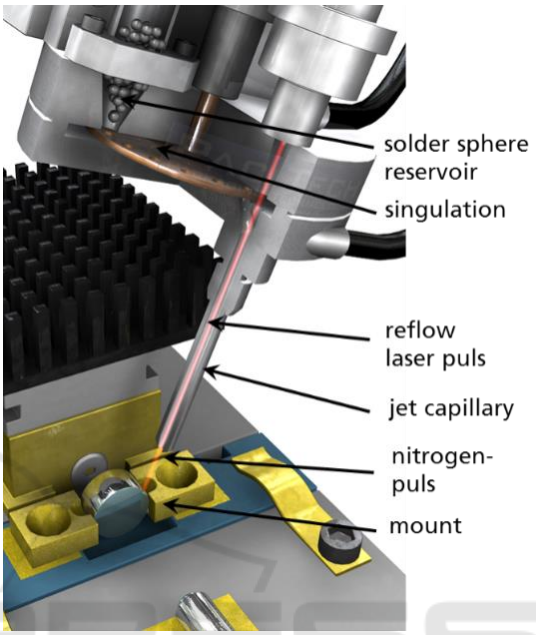

Figure 3: Solderjet bond head drawing (Ribes et al., 2018).

The surface roughness and the temperature distribution given by the thermal conductivity during the soldering are the crucial factors in determining the final wetting, the shape of the solder joint, its adhesion and the mechanical strength. A three-layer metallization system Ti/Pt/Au is locally applied on the substrates before the soldering process in a physical vapour deposition (PVD) magnetron sputtering process. Schematically, the role of every single layer is defined in Figure 4: adhesion promoter (Ti), diffusion barrier (Pt) and a wetting surface (Au):

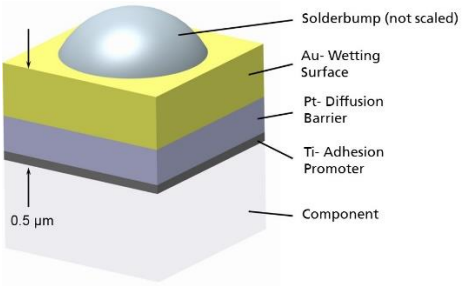

Figure 4: IOF Metallization system applied to create a wettable surface (Ribes et al., 2018).

2 REQUIREMENTS

The interest of this article was concentrated on the soldering parametrisation to assemble the optical materials for the space mission described above. This involved achieving several essential parameters, such as a good wetting (Figure 2) and high mechanical strength of the joint (mainly defined by the alloy selection).

The solder alloy has to be suitable for producing solder joints with sufficient strength and gain a high resistance to the thermal fatigue. These characteristics have to continue over the operating life of a soldered assembly and meet the rest of requirements.

While soldering, it is important to have a very local input of the thermal energy on the optical components during the die attachment process to avoid the formation of the cracks or even abrasion inside the optical components. This comes from the fact that during a long lifetime (ten years on the Earth, ten years on the orbit) cracks have a tendency to grow further under harsh environmental conditions, so the prevention of any possible damage inside the material is a priority.

The bonding alloy chosen for that specific application is based on Sn/Ag/Cu system (SAC305, 96.5 % tin, 3% silver, and 0.5% copper). It is one of the standard alloys in the electronic industries which is space qualified, and it is chosen because it displays an optimal balance which took into the consideration all the essential properties like melting temperature, strength, plasticity, fatigue life.

The stated tests are carried out with materials, which relevant characteristics are listed in Table 1 (Global solder solutions, 2018; High-temperature metals, 2018; Schott, 2018):

Table 1: Material properties.

	N-BK10	KOVAR	SAC305
Thermal conductivity, (W/mK)	1.32	17.3	58.7
Density (g/cm3)	2.39	8.36	7.49
Melting Temp (°C)	551	1450	217

The samples for the testing procedure are manufactured at Fraunhofer IOF. The investigated items are: non-coated, Ni-coated (with an applied layer of Ni 5 µm) and Ni-Au-coated (with applied layers of Ni 5 µm and Au 3 µm) KOVAR and non-coated and coated (with band-pass and antireflective coating) N-BK10. A three-layer metallization system Ti/Pt/Au is applied to all the samples, except the Ni-Au-coated KOVAR (as Au is already a wettable and noble final solderable layer). The interest of the coatings investigation is coming from a comparison of two types of manufacturing processes (conducted by IOF and by Sodern, respectively) and the need of using optical coatings for better light transmission. The selection of particularly Ni-type of the coating is explained by the motivation to prevent the possible oxidation process on KOVAR material during the storage. Assembled filters have to withstand the environmental conditions as required for the space application usage (Table 2).

Table 2: Mechanical environments.

Environments Values		
Sine vibrations	±20g	
Random vibrations	7 gRMS max (20 - 2000Hz)	
Shock	10Hz:	10g
	1000Hz-10kHz:	140 g

At the same time, these regulations shall apply in a high range of thermal cycling in the following stages (Table 3):

Table 3: Thermal environments.

Stage	Temperature range
Functional	(10°C ; 50°C)
Transport and storage	(5°C; +35°C)
Qualification	Margin ±10°C (-5°C; +60°C)

The assembling process is performed in a clean room ISO 5, as no particle bigger than 10 µm is allowed on the future sensor mode cavity.

3 ASSEMBLY EXPERIMENTAL DETAILS

In the contemplation of the aim of proving the adhesion and strength of the solder bumps (adjoining the mentioned selected materials for the filter) and in order to assess the required laser energy to attach the samples without any damage, specific tests on laser parametrisation were performed. The testing could be divided into two groups: the parametrisation tests on the samples of 20x20x5 mm size, and dummy testing, which represents the analysis of the solder behaviour

on a construction similar to the sensor module. For the whole assembly, bumps with a diameter of 400 µm were chosen due to the filter geometry (Figure 1, 5).

3.1 Dummy Design

A simplified version of the sensor module (dummy) is represented in Figure 5.

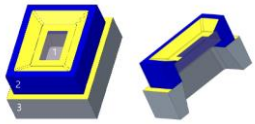

Figure 5: The dummy construction (1- N-BK10, 2-KOVAR frame, 3-KOVAR base), with an angle between N-BK10-KOVAR 30° and sidewalk between KOVAR-KOVAR of 0.3 mm.

The dimensions and geometry itself (adjoining areas between the materials to be bond) are similar to the dimensions of the final filter assembly (Figure 1). After the preliminary testing stage, this construction should be soldered with the investigated parameters to prove that the Solderjet Bumping technique can successfully assemble an optical system made of N-BK10 and KOVAR.

3.2 FEM Simulation

In order to predict the behaviour of the bound between the materials, the finite-element-method (FEM) was taking place with the help of NX9 and Nastran (SOL101, linear calculations) software. The estimation of the stress level of the heat applied to the defined geometry of the dummy was performed with a fine mesh structure, shown in Figure 6:

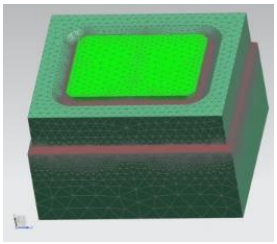

Figure 6: The view of the meshed dummy.

This numerical analysis is carried out with the following parameters, which were taken into account (Table 4):

Table 4: Required parameters for FEM (Global solder solutions, 2018; High-temperature metals, 2018; Schott, 2018; Allied Electronics and Automatics, 2018).

Material	Elastic limit (MPa)	Limit to break (MPa)	Elastic safety factor	Breaking security factor	Thermal expansion coefficient (10-6/K)
KOVAR	345		1.65		5.5
N-BK10		25		3.75	5.8
SAC 305	35	45	1.65	3.75	23.5

The test result, performed in Figure 7, revealed, that with SAC305 applied to selected materials, the following stress distribution between KOVAR-N-BK10 and KOVAR-KOVAR at a thermal load (as seen in Table 3) could be observed. It is shown, that the white areas are above the 0.875 MPa value due to the singularities of sharp edges. The thermal loads applied (as displayed in Figure 7) come from Table 3 «Thermal Environments».

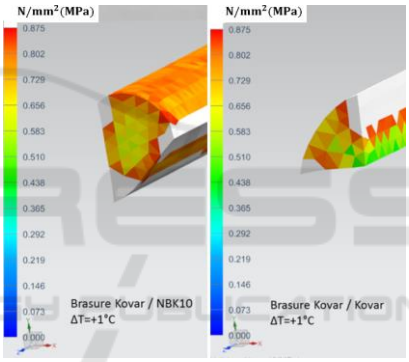

Figure 7: FEM mechanical analysis.

4 PARAMETRISATION TESTING

4.1 Parametrisation Tests on Non-Coated Materials

The purpose of the parametrisation tests, as stated above, was to achieve the good wetting of SAC305 onto the KOVAR and N-BK10 glass without damaging the bulk material. On the N-BK10 and KOVAR solder alloys (400 µm diameter) with different input energies were applied.

In each case, a Design of Experiment (DOE, D-optimal design) was created by 45 varying energy points (in terms of the laser current and the laser pulse). The diameter of the applied bumps, according to the definition of wettability, was supposed to be in the range:

$$1.25d < d_0 < 1.75d \quad (1)$$

where d_0 represents the bump diameter before melting (400 µm) and d is the melted bump diameter (Mäusezahl et al., 2016). The damage on the sample was detected via the Zeiss microscope (inspection classifying it in: no damage observed, the presence of a small crack, glass abrasion, glass bigger abrasion).

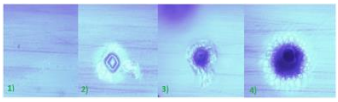

Figure 8: Types of classified damage: (1) no damage observed – blue colour on the graphs below. (2) presence of small crack - green colour on the graphs below, (3) glass abrasion - yellow colour on the graphs below (4) glass bigger abrasion - red colour on the graphs below (Ribes et al., 2018).

In Figure 9 is shown a distribution of the 45 energies with varying parameters of the laser current (A) and the pulse duration (ms), which forms the response surface plot of the input energy parameters and output parameters (in terms of the size of the bump diameter (as seen in equation 1) applied on the uncoated N-BK10):

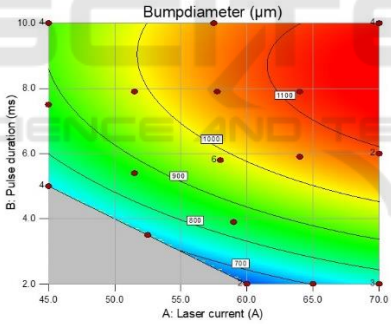

Figure 9: N-BK10 400 µm, diameter variation.

In Figure 9 is visible, that the diameter of solder bumps is varying from 600 µm to 1100 µm, depending on the energy of the laser. The green area represents the range of our interest in terms of the good solder wettability, related to equation 1.

In Figure 10, a correlation between the pulse energy (as a function of pulse duration and laser current) and the damage of the material is observed.

Furthermore, it could be derived from the Figure 10, that the values of the laser current above 55 A and laser pulse above 4 ms produce high damage on the material, consequently, all the energy examination which includes a current of the laser beam above the stated values should not be carried out.

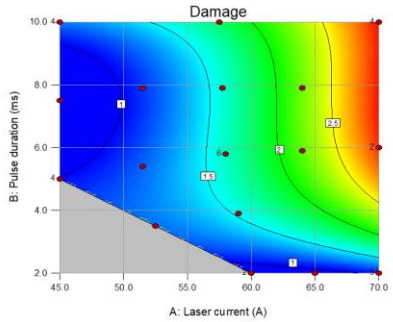

Figure 10: Damage dependence on N-BK10 (400 µm).

The same study was performed on non-coated KOVAR. The variation of the diameter is seen from Figure 11.

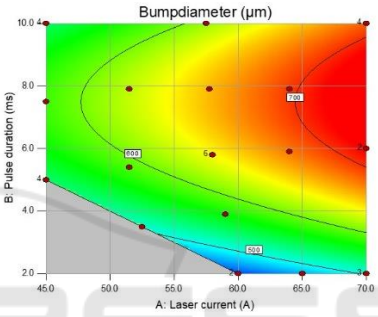

Figure 11: KOVAR 400 µm, diameter variation.

The diameter of the solder bumps, in this case, is varying from 500 µm to 700 µm, which reflects the difference between the thermal conductivity of the materials (Table 1).

The desirability is a function of both target criteria: bump diameter and damage as well. The principle of this function is maximum wetting (high bump diameter) and zero damage. The results are shown in Figure 12. The areas of the desired values are defined by colour visualisation (red represents the closer value to the desired one).

Thus, Figure 12 shows the desirable energies to bond N-BK10 and KOVAR without creating a material damaging and with providing good wetting.

The parameterisation experiments and desirability graphics revealed an acceptable soldering laser energy of~600 mJ, defined from the red area of Figure 12, which have to be applied to bond N-BK10 and KOVAR.

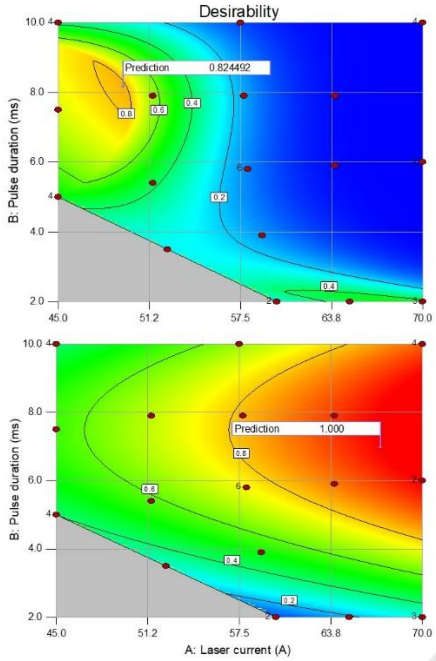

Figure 12: Up: non-coated N-BK10 (400 µm); down: non-coated KOVAR (400 µm).

4.2 Shear Tests

In this section, comparison of the shear force on coated and non-coated materials was done. Detection of the shear strength is an important second stage because most solder joints are subjected to shear stress during their service. This test reveals information about the metallization adhesion (Ti layer) and proves the wettability of the bumps over the material (Mäusezahl et al., 2016).

Preferred soldering parameters were tested on the materials by applying ten bumps of 400 µm diameter on the non-coated and coated samples (Ni-coated with Ti/Pt/Au metallization KOVAR, Ni-coated with Sodern Au metallization KOVAR and also N-BK10 with band-pass and antireflective coating, respectively).

Before the shear test, additional visual inspection of the bumps was performed. In the case of KOVAR Ni-Au, the diameter of the bump was larger than on the non-coated KOVAR (with the same laser reflow energy applied). This is coming from the difference of the roughness of the surfaces and means that the samples with the coating are easy to solder due to a better wettability surface (dummy components were manufactured at different facilities: Fraunhofer IOF or Sodern). The contrast between Ni-Au and Ni-Ti/Pt/Au coating on KOVAR was only in 5% of variation in the diameter value, so it was considered, that both KOVAR coatings are acceptable for the project, and the easier one to be applied (in terms of time/cost) is selected for the final assembly. The results of non-coated and coated N-BK10 gave the same tendency of the solder behaviour. On the N-BK10 with applied band-pass coating the bump diameter was slightly smaller (around 7 %) than on the antireflective one.

4.2.1 Shear Tests on KOVAR

The melted area was examined via the Zeiss microscope to reveal the quality of the metallization for the KOVAR Ni- Ti/Pt/Au and KOVAR Ni-Au. All the remaining bumps had the same area, so the results showed a proper adhesion on the applied surfaces and high repeatability (Figure 13).

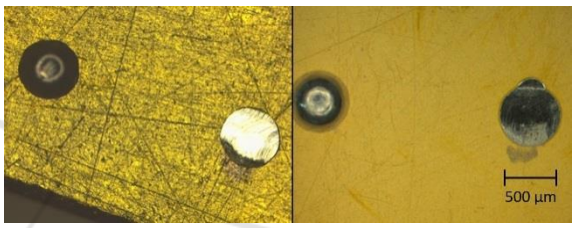

Figure 13: The shear test (before and after) on KOVAR Ni-Ti/Pt/Au and KOVAR Ni-Au.

The dynamics of the shear force over time is shown in Figure 14, an increase of the melted area led to the increase of the shear force.

The shear force was tested using a FS Automatic Bonder and Tester with a SH-5000 head.

Figure 14: The evolution in time of the shear force for the 400 µm bump: the graphic starts from the moment of the touchdown of the needle onto the solder alloy, then the force is increasing and reaching its maximum in the middle of the bump, afterwards, symmetrically decreasing again. The laser current is 49.5 A, the pulse duration is 8.2 ms, test is conducted in a room temperature of 23°C.

The shear force values were detected independently for each bump. In general, the values depend on a variety of factors, such as thermal conductivity, shear rate (high/slow), the energy of the applied pulse, the temperature of samples of the

performed test (Mäusezahl et al., 2016). Taking all this into account, the estimated theoretical values supposed to be in the range of 1000-1300 cN. For KOVAR, the value (Figure 14) fits this expected range.

4.2.2 Shear Tests on N-BK10

The investigations on non-coated and coated (antireflective – AR, band-pass – BP) N-BK10 samples were performed with the parameters of the laser current and pulse, defined above. The test revealed that the AR or BP coating on the N-BK10 is not resulting in differences on bump adhesion. A visual inspection was arranged for both samples (Figure 15).

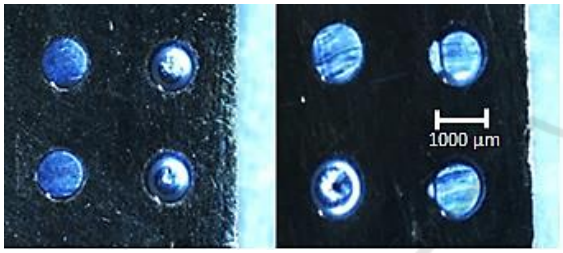

Figure 15: Comparison of solder and shear drops: left: BP; right: AR.

It was concluded, that both types neither enhance, nor degenerate an acceptable solder behaviour. On the next step, during the shear test, the shear force (over time) was measured on each bump. This additional attention comes from the properties of the glass material and requirement of no damage inside for the further assembly (Table 5):

Table 5: The average (av.) shear force for both coatings.

N-BK10, 400 µm (BP)		N-BK10, 400 µm (AR)	
Av. square, μm^2	Av.force, cN	Av. square, μm^2	Av. force, cN
817	1043	803	994

N-BK10 (BP) gave closer results to the expected shear force values (for the melted diameter and parameters, discussed above in section 4.2.1). In the case of N-BK10 (AR), the achieved shear force was less than the predictable one from the defined above range. However, as this difference is not sufficient, both coated and non-coated materials are acceptable for the project.

4.3 Pitch fixation

In order to study the distance between the soldering bumps (pitch) and achieve a device with high strength, adjustment test was conducted. Bumps of 400 µm diameter were applied in one raw (with a fixed distance between them) on the N-BK10 and KOVAR.

The testing was done to find an optimal overlapping spacing between the materials, so that the resulted pitch has to be a continuous line of solder bumps, which do not create any cracks inside the surface. KOVAR Ni-Au showed almost equal results as KOVAR Ni-Ti/Pt/Au, but bumps on KOVAR Ni-Ti/Pt/Au tended to be a bit larger than on KOVAR Ni-Au (the pitch on KOVAR Ni-Au has to be smaller). On the two types of N-BK10 coatings, the difference was undetectable.

4.4 Dummy Soldering

The dummy with dimensions similar to the filter was manufactured at Fraunhofer IOF to prove the stated parameterisation. The soldering was applied between N-BK10 window and KOVAR frame and between KOVAR frame and KOVAR base, as defined above. The microscope investigation revealed, that on the optical glass, manufactured at IOF, some cracks were observed before the bonding process. The reason for this was the difficulty of achieving the properly polished glass edges on the NBK10 (required factor was P4). However, soldering process itself did not produce any damage.

5 CONCLUSIONS

The primary objective of this study was to highlight the challenges of using a Solderjet Bumping technique for the assembling of a new generation of optical filters. The tests have shown that for a successful bound of the components, the energy of the laser pulse should be in the range of 600 mJ and these results proved no damage, even in the sensitive glass material. Moreover, the soldering strength guarantees a final strength of alloying to pass the environmental and mechanical requirements.

The shear test has verified the quality of the applied metallization layers (both, Sodern and IOF). Metallization difference in KOVAR Ni-Au (by Sodern) or KOVAR Ni-Ti/Pt/Au (by IOF) did not perform a significant influence on the material response to the developed parameterisation values.

Thus, the materials, required for the space mission (N-BK10 and KOVAR), can be successfully soldered with SAC305 alloy.

The continuous soldering on the dummies revealed the growth of the cracks (done by not perfectly polished surface) inside the optical glass, so another design approach was elaborated.

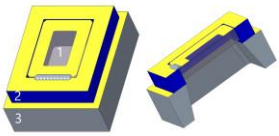

Figure 16: Another design approach: KOVAR frame (2), N-BK10 filter (1).

The main advantage of the design lays in the reduction of the possible thermal shock on the optical glass due to the homogeneously spreading solder alloy on the perfectly polished surface, which quality is not that hard to achieve as on the edges before (Figure 16). Moreover, preventing the damage formation while manufacturing and reducing the metallization costs (due to the decrease of the number of required runs, only one is required now) are the main achievements of the new elaboration.

Furthermore, the initial soldered dummies (Figure 17) went through the thermal environmental testing (-40°C, 150°C), and the results performed excellent stability for soldering as no evolution concerning the cracks already present were observed.

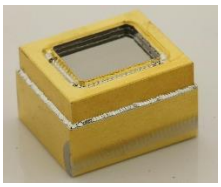

Figure 17: The soldered dummy.

Thus, due to this successful outcome (in terms of the high-quality bond between the examined materials and no damage revealed), the defined above parameterization is recommended for the optical filter module, consisting of the two mentioned assemblies, which is a significant improvement for the construction of the new generation of the filter for the space missions.

ACKNOWLEDGEMENTS

This research work is funded by a European space instrument provider - Sodern.

REFERENCES

Le Goff, R., Pranyies, P., Toubhans, I. (2006), Focal plane AIT sequence: evolution from HRG – Spot 5 to Pleiades HR, *Proc.6th International Conference on Space Optics, ESTEC, Noordwijk, The Netherlands, 27-30 June 2006 (ESA SP-621).*

Airbus (2017), *Airbus to reshape Earth observation market with its Pléiades Neo constellation* (online). Available at:*https://www.airbus.com/newsroom/press-releases/en/2017/09/Press-release-SpaceDataHighway.html* (Accessed 12 Nov.2018).

Gleyzes, A. and Perret, L. (2013), Pleiades high resolution optical earth observation system status and future missions preparation in the frame of OTOS CNES program, *64th International Astronautical Congress, Beijing, China.*

Pranyies, P., Toubhans, I., Badoil, B., Tanguy, F., Descours, F. (2018), *Focal plane for the next generation of earth observation instruments*, 1st ed. (pdf). Available at: www.sodern.fr (Accessed 12 Nov. 2018).

Brockmann, W., Geiß, P.L., Klingen, J., Schröder, B. (2009), *Adhesive Bonding: Materials, Applications and Technology*, Weinheim: Wiley-VCH.

Wagner P. (2014), *Laser-induced contamination on high-reflective optics*, Master Thesis, University of Applied Science Darmstadt and DLR- German Aerospace Center.

Wernham D., Alves J., Pettazzi F., Tihe A.P. (2010), "Laser-induced contamination mitigation on the ALADIN laser for ADM-Aeolus", in Proceedings of SPIE, *Vol. 7842*; Available from: doi:*10.1117/12.867268*.

Ribes, P., Bruckner, G., Beckert, E., Eberhardt, R., Tünnermann, A. (2018), Lithiumniobate Die Assembled by a Low-stress Soldering Technique, Method to Fasten a Surface Acoustic Wave Sensor, *6th International Conference on Photonics, Optics and Laser Technology (PHOTOPTICS 2018)*, pages 91-97.

Ribes, P., Koechlin, C., Hornaff, M., Kamm, A., Beckert, E., Fiault, G., Eberhardt, R., Tünnermann, A. (2016), High-precision optomechanical lens system for space applications assembled by a local soldering technique, *Opt. Eng. 55(6), 065101 (2016)*, Available from: doi*: 10.1117/1.OE.55.6.065101.*

Puttlitz, K.J. and Stalter, K.A. (2004), *Handbook of Lead-Free Solder Technology for Microelectronic Assemblies*, New York: Marcel Dekker.

Global solder solutions (2018), *Technical data sheet SAC305 lead-free solder alloy* (online). Available at: *https://www.aimsolder.com/sites/default/files/alloy_sac305_tds.pdf* (Accessed 12 Nov.2018).

High temperature metals (2018), *Kovar technical data* (online). Available at: *http://www.hightempmetals.com/techdata/hitempKovarrdata.php* (Accessed 12 Nov.2018).

Schott (2018), *Datenblatt N-BK10* (online). Available at: *https://www.schott.com/advanced_optics/german/abbe*

_datasheets/schott-datasheet-n-bk10.pdf (Accessed 12 Nov.2018).

Allied Electronics and Automatics (2018), *Lead Free Solder Sn96 (SAC 305)* (online). Available at: *https://www.alliedelec.com/m/d/8d9ef1f686bf70839a288bf4fd8e669e.pdf* (Accessed 31 Dec.2018).

Mäusezahl, M., Hornaff, M., Burkhardt, T., Beckert, E. (2016), Mechanical properties of laser-jetted SAC305 solder on coated optical surfaces, *Physics Procedia, Vol. 83, p. 532-539, Elsevier.*